1996

Analysis of Oil Film at Vane Side in Vane Compressors

M. Fukuta
Shizuoka University

T. Yanagisawa
Shizuoka University

T. Shimizu
Shizuoka University

ANALYSIS OF OIL FILM AT VANE SIDE IN VANE COMPRESSORS

Mitsuhiro FUKUTA, Tadashi YANAGISAWA and Takashi SHIMIZU

Department of Mechanical Engineering, Shizuoka University,
3-5-1, Johoku, Hamamatsu, 432, JAPAN

ABSTRACT

In order to utilize HFC refrigerant, which is said to make lubricating condition worse, as a working fluid in a refrigeration cycle, it is needed to evaluate the lubricating condition at sliding parts accurately. In this study, we analyzed oil film at vane sides in a vane compressor with a hydrodynamic lubrication theory. We also analyzed the vane behavior, frictional loss on the vane side and leakage flow through these clearances under steady-state operating condition. It is clarified that the inclination of the vane in a vane slot of a rotor changes with rotor rotation and the vane is pressed strongly on its trailing side against an edge of the vane slot when pressure of working fluid in compression chamber approaches discharge pressure. The calculated results of vane behavior and contact forces are influenced by method of modeling of the oil film pressure under the condition that the vane comes into contact with the rotor.

INTRODUCTION

In order to utilize HFC refrigerant, which is said to make lubricating condition worse, as a working fluid in a refrigeration cycle, many studies concerning lubrication and wear have been done. Most of the studies discussed about compatibility and wear of materials and elasto-hydrodynamic lubrication (EHL) conditions, but a hydrodynamic lubrication theory is also useful due to its simplicity as the first step to evaluate influences of clearance, oil viscosity and operating condition on the lubricating condition. In this study, we analyzed oil film at vane sides in a vane compressor with the hydrodynamic lubrication theory. We also analyzed vane behavior, frictional loss on the vane side and leakage flow through these clearances under steady-state operating condition. At that time, three models of oil film pressure under the condition that the vane comes into contact with a vane slot of a rotor are proposed and the results with these models are compared with each other.

THEORETICAL ANALYSIS

In this study, we applied the hydrodynamic lubrication theory to the oil film at the vane sides in the vane compressor and analyzed the vane behavior and contact forces under steady-state operating condition.

Lubrication Model of Oil Film at Vane Side

Figure 1 shows a schematic view of the vane compressor for an automotive air conditioner and Fig. 2 shows a lubrication model of oil film at the vane side. The followings are assumed for simplicity. (1)Sliding portion has infinite width. (2)Lubricant is incompressible and its viscosity is constant. (3)Inertial force of lubricant is negligible. (4)Deformations of the vane and the vane slot of rotor are negligible. (5)Rotational speed of the rotor is constant.

Relationship between pressure, P, of oil film and clearance height, h, on coordinates system shown in Fig. 2, which move with the vane, is expressed by the Reynolds equation as follows.

$$\partial\left\{h^3\left(\partial P/\partial x\right)\right\}/\partial x = -6\eta U\,\partial h/\partial x + 12\eta\,\partial h/\partial t \qquad (1)$$

Where, η:viscosity of oil, U:velocity of vane, x:position on abscissa , t:time. We express the variables of clearance height, h, and its time differential, $\partial h/\partial t$, with clearance, h_0 , at origin and inclination, k, of the vane /1,2/ as follows.

$$h = h_0 + kx \qquad (2)$$

$$\partial h/\partial t = dh_0/dt + x\,dk/dt \qquad (3)$$

Integrating Eq. (1) under the following boundary conditions,

$$P_{(x=0)} = P_0, \quad P_{(x=L)} = P_1 \tag{4}$$

then we obtain the oil film pressure distribution in the clearance as follows.

$$P = A_{11}\, dk/dt + A_{12}\, dh_0/dt + A_{13}U + A_{14}P_0 + A_{15}P_1 \tag{5}$$

Where, coefficients, A_{ij}, of each term in Eq. (5) are function of the clearance height, h, at position x, clearance heights, h_0, h_1, at the both ends of held portion of the vane by the vane slot, inclination, k, the held length of vane, L, and oil viscosity, η, as shown in appendix. Forces and moments acting on the vane due to the oil film pressure and oil shearing forces are derived based on the pressure distribution. (note that direction of shearing force is negative of x.)

$$F_s = \int_0^L P dx = A_{21}\, dk/dt + A_{22}\, dh_0/dt + A_{23}U + A_{24}P_0 + A_{25}P_1 \tag{6}$$

$$M_s = \int_0^L xP dx = A_{31}\, dk/dt + A_{32}\, dh_0/dt + A_{33}U + A_{34}P_0 + A_{35}P_1 \tag{7}$$

$$F_\tau = \eta \int_0^L \left(\partial u/\partial y\right)_{y=h} dx = A_{41}\, dk/dt + A_{42}\, dh_0/dt + A_{43}U + A_{44}P_0 + A_{45}P_1 \tag{8}$$

Coefficients, A_{ij}, are shown in appendix. Concerning the opposite clearance of the vane side, we can obtain similar equations by substitution of variables: $h_0 \to h_0'$, $h_1 \to h_1'$, $L \to L'$ $k \to -k$, $dh_0/dt \to -dh_0/dt$, $dk/dt \to -dk/dt$, respectively.

In this study, we considered not only the case when the vane does not contact with the vane slot of the rotor (= fully hydrodynamic lubricating condition), but also the case when it comes into contact with the vane slot. In the case of the contact condition, we modeled the pressure of oil film in the following three cases and compared the results with each other. In case 1 it is assumed that there exists a minimal clearance at contact point due to surface roughness even if the vane has contacted with the vane slot. then the lubrication theory described above can be applied. Case 2 assumes that the pressure distribution is discontinuous at the contact point, so the pressure in the clearance is equal to boundary pressure at non-contact side. On the other hand, in case 3 we considered only squeeze effect which is generated when the vane inclination changes. When the clearance h_0 in Fig. 2 becomes smaller than a certain value and the vane has contacted with the vane slot, the pressure distribution due to squeeze effect under this condition is given by the next equation.

$$P = \frac{6\eta}{k^3}\left\{\log\frac{h}{h_1} + \frac{2h_0}{h} - \frac{h_0^2}{2h^2} - \frac{h_0(4h_1 - h_0)}{2h_1^2}\right\}\frac{dk}{dt} + P_1 \tag{9}$$

In case of the clearance h_1 becomes smaller than that certain value and the vane comes into contact with the vane slot at h_1 side, subscripts 0 and 1 will be swapped with each other in Eq.(9). Forces and moments acting on the vane due to the oil film pressure and oil shearing forces are derived in the similar way based on Eq.(9).

Vane Behavior and Contact Forces

Figure 3 shows forces acting on the vane. By taking account of such forces as centrifugal force, F_r, inertia force, F_i, coriolis force, F_c, pressure forces of gas, F_p, F_{pt}, force, F_b, due to backpressure of vane, contact and frictional forces, $F_n, \mu F_n$, at vane tip, forces, $R, \mu R$, due to contact and friction with rotor, pressure forces, F_s, of oil film and oil shearing forces, F_τ, and also by taking account of moment around vane bottom due to each force, we obtained balancing equations of forces (X ,Y direction) and moments.

$$F_{rx} + F_c - F_s + F_s' - F_p + F_p' - F_n(\cos\gamma - \mu_t \sin\gamma) + c_0 R_0 + c_1 R_1 = 0 \tag{10}$$

$$F_b + F_{ry} - F_i - F_{pt} - F_{pt}' - F_\tau - F_\tau' - F_n(\sin\gamma + \mu_t \cos\gamma) - i\mu_s(R_0 + R_1) = 0 \tag{11}$$

$$\begin{aligned} M_p - M_p' - M_{pt} + M_{pt}' + M_s - M_s' - M_\tau + M_\tau' - M_{rx} - M_c + c_0 R_0 i\mu_s t_v/2 + c_1 R_1\left(i\mu_s t_v/2 - L^*\right) \\ + F_n\left\{(\cos\gamma - \mu_t \sin\gamma)(L + L_t) - (\sin\gamma + \mu_t \cos\gamma)(X_v - a)\right\} = 0 \end{aligned} \tag{12}$$

Where, μ:frictional coefficients at vane tip and vane side, L_t :vane extension length, t_v :vane thickness, X_v: ordinate of contact point at vane tip, a :vane offset, γ:angle of normal line at vane tip contact point from X axes, ':leading

side of vane. Coefficient c_0, c_1 equal to 1 when the vane comes into contact with the rotor at leading side, and equal to -1 when it comes into contact at trailing side. Coefficient i equals to 1 when the vane velocity is positive, and equals to -1 when negative. L^* equals to L' when the vane comes into contact with rotor at edge of vane slot of leading side, and equals to L when it comes into contact at the opposite edge of vane slot. In Eqs.(10)-(12), velocity and acceleration of vane are given geometrically and pressure in compression chambers are given by assumption of adiabatic compression based on geometric volume change of compression chamber. The forces of oil film are given as described in the previous section. By the way, when the vane does not contact with the rotor the contact forces at the vane side become 0, and when it comes into contact its behavior is restricted by the vane slot. So the following boundary conditions are made up according to the condition of contact or non-contact of the vane with the rotor.

·At vane bottom	Contact	$dh_0/dt = 0$	
	Non-contact	$R_0 = 0$	(13)
·At edge of vane slot	Contact	$L\,dk/dt + dh_0/dt - Uk = 0$	
	Non-contact	$R_1 = 0$	(14)

By solving Eqs.(10)-(14) simultaneously, we can calculate the time differential of the inclination, dk/dt, of the vane, time differential of the clearance height, dh_0/dt, contact force, F_n, at the vane tip and contact forces, R_0, R_1, at the vane side.

The vane behavior is calculated by the Runge-Kutta method with an initial position of the vane assumed arbitrarily and the calculation is iterated until the vane behavior is converged. In the calculation, it is assumed that the vane comes into contact with the rotor when the clearance becomes less than 1 μm by taking surface roughness into account. Specifications of the compressor and conditions of calculation are listed in Table 1. Since the vane side is treated as the slider having infinite width in the calculation, the following results are described by values per unit width.

RESULTS AND DISCUSSION

Figure 4 shows relationship between rotational angle and pressures in the compression chamber, which will be used in the later calculation. Where, P_1' is the pressure in the compression chamber leading to the vane and P_1 is that in the trailing chamber. They contains effects of over compression, re-expansion at discharge port and leakage through axial seal. In addition, the backpressure of vane, P_0, is assumed to be constant.

Figure 5 shows changes of the clearances at the vane side and the contact forces with the rotor in 1 cycle of rotation, and the pressure distribution on the vane side at rotational angle of $4\pi/3$ rad. Three lines shown in Fig. 5 are the results corresponding to three lubrication models of oil film at the vane side under the contact condition, i.e., solid line is for the case 1, dotted line is for the case 2 and chain line is for the case 3. It is found that the vane inclines toward trailing side of a rotating direction at rotational angle of 0 rad and inclines toward the opposite side during the first half of rotation due to the contact force acting on the vane tip. After that, as the pressure in the compression chamber increases the vane inclines toward the former direction again and the vane is pressed strongly against the edge of vane slot when pressure of working fluid in compression chamber approaches discharge pressure. Though there is little difference among the vane behavior for three cases of lubrication model under the contact condition, the contact force in the case 1 is the largest and that in the case 3 is the smallest among them. The difference of contact force reflects the different pressure distribution on the vane side. As shown in Fig. 5 the pressure distribution on the vane side at the rotational angle of $4\pi/3$ rad in case 1 has a negative value near the end of the vane slot due to reverse wedge effect. On the other hand, pressure near the end of vane slot in case 3 is high due to squeeze effect. In this analysis when the pressure is negative, we calculate the pressure forces and moments by neglecting the negative value. By the way in the calculations of case 2 and case 3, there is the case occasionally that the calculated result becomes the contact condition of the vane under the assumption of non-contact condition, or conversely it becomes the non-contact condition under the assumption of contact condition, so the condition of contact or non-contact can not be decided. This is because the lubrication model of oil film at the vane side used in the calculation is changed according to the condition of contact or non-contact. For these cases, the vane is assumed to come into contact with the rotor, the vane behavior is restricted and the contact force is made to be 0. For the calculation of case 1, on the other hand, continuous calculation can be done because there is no switch of the

lubrication model.

Figure 6 shows the result when the viscosity of lubricant is low. Compared with the results shown in Fig. 5, it is found that a motion of the vane in the vane slot is large. The result of case 2 is not shown in Fig. 6 because of the following reason. When the inclination of the vane becomes small under the contact condition with the rotor at one side, which occurs at rotational angle about $3\pi/2$ rad, the vane approaches one side of the vane slot because the pressure on the contact side is constant regardless of the vane behavior and then it is not possible to calculate by this analysis. There is little difference between the results of the contact forces for case 1 and case 3 because the pressure generation of oil film is small due to small viscosity of lubricant. The pressure distribution on the vane side, therefore, is almost the same for both cases as shown in Fig. 6. When the pressure generation of oil film is large (large viscosity, high rotational speed and small clearance), conversely, experimental verification of the pressure distribution under the contact condition is needed since the calculated contact forces are much affected by the modeling of lubricating oil film. Comparing the analytical result with an abrasion mark on the vane of the compressor which has been operated for a long time, analysis of contact range seems to be appropriate, but degree of wear is a little different from the calculated contact force. It is, therefore, needed to take the contact force, contact angle, sliding speed, characteristics of lubricant, etc. into account in order to evaluate the vane's wear.

This analysis also can estimate leakage flow rate of oil through the vane side clearance into the compression chamber by using the pressure gradient at the end of vane slot. Figure 7 shows the leakage flow rates through the clearance leading to the vane (G') and through the clearance trailing to the vane (G) for different oil viscosities. In the case of low viscosity oil, the leakage increases at the rotational angle of π rad as the clearance leading to the vane increases.

Figure 8 shows the torque generated by frictional loss at vane side with the rotational speed of 1,000 rpm and 3,000 rpm. The torque is calculated by multiplying the summation of frictional force and oil shearing force by the extension velocity of vane, and then dividing by rotational angular velocity. The torque shown in this figure are summation of all losses for each vane. The frictional loss due to the contact between the vane and the rotor is much larger than that due to the oil shearing force. The loss at the higher rotational speed is larger than that at the lower rotational speed, this is because the contact range increases with increasing of rotational speed.

Although we use the analysis to evaluate the lubrication condition at the vane side of the vane compressor in this paper, the analysis is applicable to any sliding portion consisting of a plane and a slider.

CONCLUSIONS

We analyzed the oil film at vane sides in the vane compressor with the hydrodynamic lubrication theory. We also analyzed the vane behavior, frictional loss on the vane side and leakage flow through these clearances under steady-state operating condition. It is clarified that the inclination of the vane in the vane slot changes with the rotor rotation. The trailing side of the vane is pressed strongly against the edge of vane slot when the pressure of working fluid in the compression chamber approaches the discharge pressure. The calculated vane behavior and contact forces are influenced by method of modeling of the oil film pressure under the contact condition. Although further investigation is needed for the modeling under the contact condition, the analytical method derived in this study makes it possible to analyze the vane behavior and the contact forces by taking account of the clearance, operating condition and oil viscosity. Furthermore, the analysis is applicable to any sliding portion consisting of a plane and a slider.

APPENDIX

$$A_{11}=\frac{6\eta}{k^3}\left\{\log\frac{h}{h_0}-\frac{h_1^2}{(h_0+h_1)kL}\left(1-\frac{h_0^2}{h^2}\right)\log\frac{h_1}{h_0}-\frac{2h_0^2h_1}{h^2(h_0+h_1)}+\frac{2h_0}{h}-\frac{2h_0}{h_0+h_1}\right\},\qquad A_{12}=\frac{12\eta}{k^2}\left\{\frac{h_0h_1}{h^2(h_0+h_1)}-\frac{1}{h}+\frac{1}{h_0+h_1}\right\}$$

$$A_{13}=-kA_{12}/2,\qquad A_{14}=\frac{h_0^2}{(h_0+h_1)kL}\left(\frac{h_1^2}{h^2}-1\right),\qquad A_{15}=\frac{h_1^2}{(h_0+h_1)kL}\left(1-\frac{h_0^2}{h^2}\right)$$

$$A_{21}=\frac{6\eta}{k^4}\left\{\frac{2h_0(h_0+2h_1)}{h_0+h_1}\log\frac{h_1}{h_0}-\frac{4h_0kL}{h_0+h_1}-kL\right\},\qquad A_{22}=\frac{12\eta}{k^3}\left(\frac{2kL}{h_0+h_1}-\log\frac{h_1}{h_0}\right)$$

$$A_{23}=-k\,A_{22}/2,\qquad A_{24}=h_0L/(h_0+h_1),\qquad A_{25}=h_1L/(h_0+h_1)$$

$$A_{31}=\frac{6\eta}{k^3}\left\{\left[\frac{h_1}{(h_0+h_1)k}\left(\frac{h_0^2h_1}{k^2L}\log\frac{h_1}{h_0}-\frac{3h_0^2}{k}-\frac{h_1L}{2}\right)-\frac{5h_0^2}{2k^2}+\frac{L^2}{2}\right]\log\frac{h_1}{h_0}+\frac{2h_0^2L}{(h_0+h_1)k}-\frac{h_0L^2}{h_0+h_1}+\frac{5h_0L}{2k}-\frac{L^2}{4}\right\}$$

$$A_{32}=\frac{12\eta}{k^3(h_0+h_1)}\left\{\frac{h_0}{k}(h_0+2h_1)\log\frac{h_1}{h_0}-\frac{L}{2}(5h_0+h_1)\right\},\quad A_{33}=-k\,A_{32}/2$$

$$A_{34}=\frac{h_0^2}{(h_0+h_1)kL}\left(\frac{h_1^2}{k^2}\log\frac{h_1}{h_0}-\frac{h_1L}{k}-\frac{L^2}{2}\right),\qquad A_{35}=\frac{h_1^2}{(h_0+h_1)kL}\left(-\frac{h_0^2}{k^2}\log\frac{h_1}{h_0}+\frac{h_0^2L}{kh_1}+\frac{L^2}{2}\right)$$

$$A_{41}=\frac{6\eta}{k^3}\left(-\frac{2h_0h_1+h_0^2}{h_0+h_1}\log\frac{h_1}{h_0}+\frac{2h_0kL}{h_0+h_1}+\frac{kL}{2}\right),\qquad A_{42}=\frac{6\eta}{k^2}\left(-\frac{2kL}{h_0+h_1}+\log\frac{h_1}{h_0}\right)$$

$$A_{43}=\frac{\eta}{k}\left(\frac{6kL}{h_0+h_1}-2\log\frac{h_1}{h_0}\right),\qquad A_{44}=-h_0h_1/(h_0+h_1),\qquad A_{45}=h_0h_1/(h_0+h_1)$$

REFERENCES

(1)H.Kobayashi and S.Ota, Mitsubishi Heavy Industries Tech. Report, Vol.26, No.3, (1989), 195. (in Japanese)
(2)M.Fukuta, et.al., Trans. JSME (Series B), Vol.57, No.538, (1991), 2007. (in Japanese)

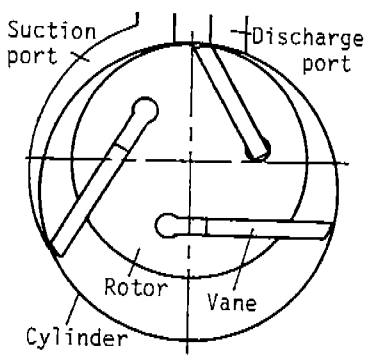

Fig. 1 Schematic view of vane compressor

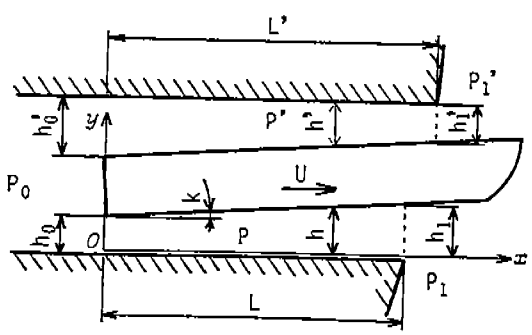

Fig. 2 Lubrication model of oil film at vane side

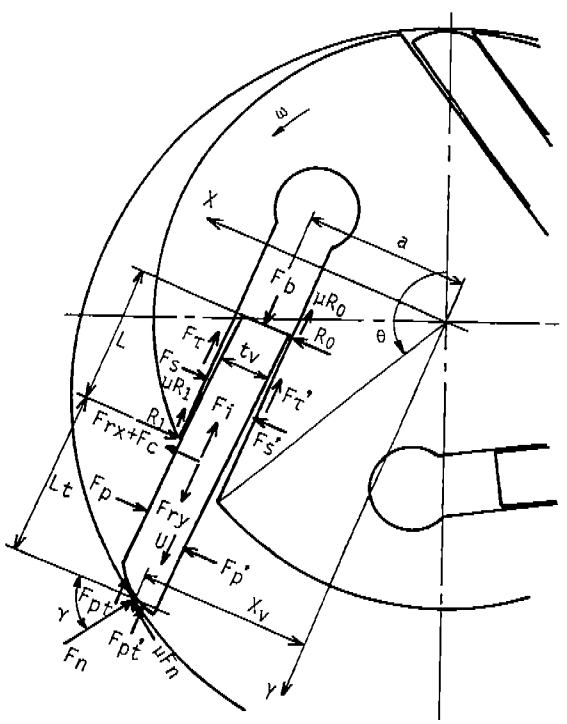

Fig. 3 Forces acting on vane

Table 1 Specifications of compressor and calculating conditions

Cylinder radius	36.3 mm
Rotor radius	28.2 mm
Vane length	31.4 mm
Vane mass per unit length	0.36 g/mm
Suction pressure	0.309 MPa
Discharge pressure	1.52 MPa
Backpressure	1.06 MPa
Vane side clearance	40 μm
Coefficient of friction	0.1

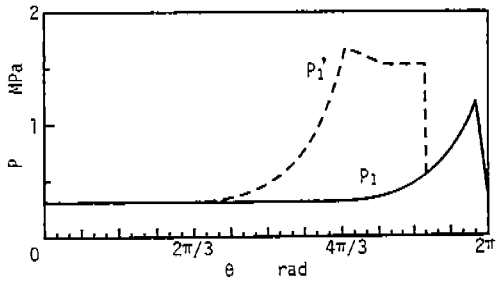

Fig. 4 Pressure change in compression chamber

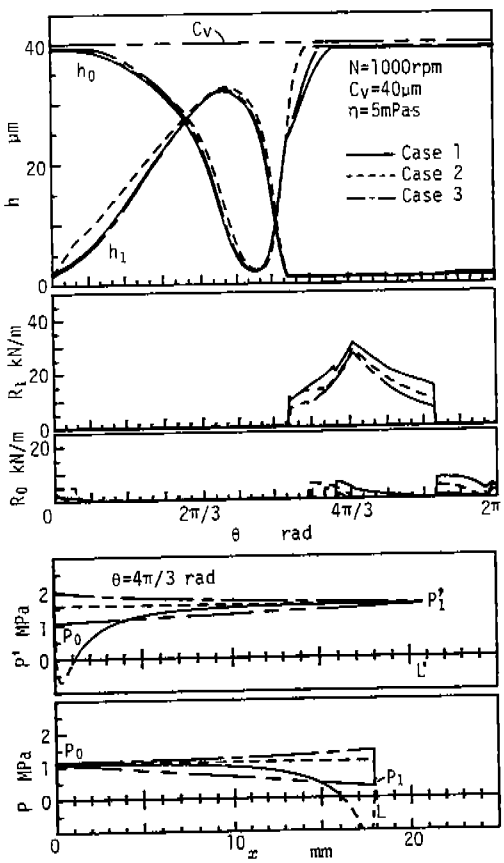

Fig. 5 Vane behavior, contact force and pressure distribution on vane side

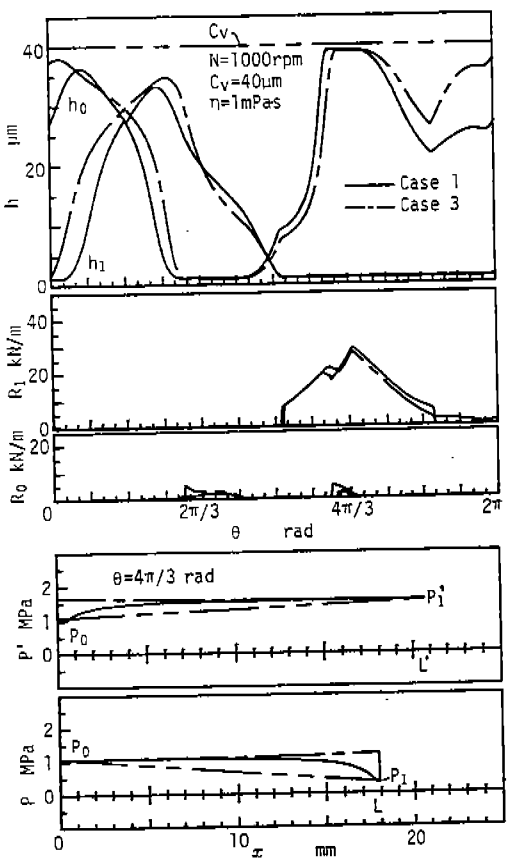

Fig. 6 Vane behavior, contact force and pressure distribution on vane side (Low viscosity oil)

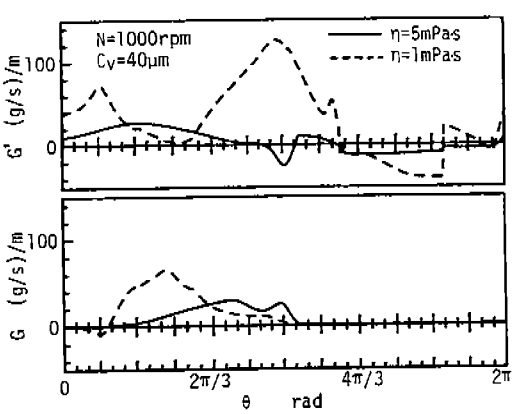

Fig. 7 Leakage flow rates through vane sides

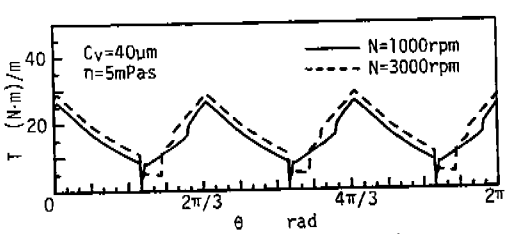

Fig. 8 Torque by frictional loss at vane side